Journal of Hepatocellular Carcinoma Dovepress

Open Access Full Text Article ORIGINAL RESEARCH

scRNA-Seq Analysis Revealed CAFs Regulating HCC Cells via PTN Signaling

Wenxian Lin[1–4], Lizhu Tang[1,2,5], Chenyi Zhuo[1], Xiuli Mao[1–4], Jiajia Shen[6], Shaoang Huang[3], Shangyang Li[3,7], Yujuan Qin[3,4], Ju Liao[2,3], Yuhong Chen[8], Xiamin Zhang[3,4], Yuting Li[9], Jian Song[4], Lingzhang Meng[4], Xiaofeng Dong[10], Yueyong Li[2]

[1]Key Laboratory of Molecular Pathology for Hepatobiliary Diseases of Guangxi, Affiliated Hospital of Youjiang Medical University for Nationalities, Baise, 533000, The People's Republic of China; [2]Department of Interventional Oncology, Affiliated Hospital of Youjiang Medical University for Nationalities, Baise, 533000, The People's Republic of China; [3]Graduate School, Youjiang Medical University for Nationalities, Baise, 533000, The People's Republic of China; [4]Institute of Cardiovascular Sciences, Guangxi Academy of Medical Sciences & The People's Hospital of Guangxi Zhuang Autonomous Region, Nanning, 530016, The People's Republic of China; [5]Department of Radiation Oncology, The First Affiliated Hospital of Jinan University, Guangzhou, 510632, The People's Republic of China; [6]Department of Laboratory Medicine, Nanning Maternity and Child Health Hospital & Nanning Women and Children's Hospital, Nanning, 530011, The People's Republic of China; [7]Department of Laboratory Medicine, Guangxi Academy of Medical Sciences & The People's Hospital of Guangxi Zhuang Autonomous Region, Nanning, 530016, The People's Republic of China; [8]Department of Nephrology, the Second Affiliated Hospital of Guangxi Medical University, Nanning, 530007, The People's Republic of China; [9]Graduate School, Guangxi University of Chinese Medicine, Nanning, 530200, The People's Republic of China; [10]Department of Hepatobiliary, Pancreas and Spleen Surgery, Guangxi Academy of Medical Sciences & The People's Hospital of Guangxi Zhuang Autonomous Region, Nanning, 530016, The People's Republic of China

Correspondence: Yueyong Li; Xiaofeng Dong, Email 305017674@qq.com; gandanyingcai@163.com

Background: Cancer-associated fibroblasts (CAFs) play a pivotal role in shaping the microenvironment of hepatocellular carcinoma (HCC). However, the mechanisms through which CAFs influence the progression of HCC remain incompletely understood.

Methods: Single-cell RNA sequencing datasets (GSE158723 and GSE112271) were retrieved from the Gene Expression Omnibus (GEO) database at the National Center for Biotechnology Information (NCBI) and analyzed using R software. Our analysis suggested that CAFs may promote liver cancer cell development, possibly through the interaction of pleiotrophin (PTN) and syndecan-2 (SDC2). Clinical samples from HCC patients were collected and processed into frozen sections and single-cell suspensions for Masson staining, immunofluorescence staining, and flow cytometry. Additionally, Huh7 liver cancer cells and LO2 normal liver cells were cultured and subjected to immunofluorescence assays using cell slides.

Results: The proportion of CAFs in cancerous tissues was higher than in adjacent non-cancerous tissues, and pleiotrophin (PTN) expression was elevated in cancer tissues compared to adjacent tissues. These findings aligned with the results of the single-cell RNA sequencing (scRNA-seq) analysis. Furthermore, SDC2 expression was significantly upregulated in Huh7 liver cancer cells compared to LO2 normal liver cells.

Discussion: This study suggests that CAFs may contribute to HCC progression via the PTN/SDC2 signaling pathway. Our findings provide deeper insights into the interactions between CAFs and HCC cells within the tumor microenvironment (TME).

Keywords: CAFs, HCC, PTN, scRNA-seq, TME

Introduction

Liver cancer poses a significant challenge. Since 2018, 841,000 new liver cancer cases have been reported worldwide, making it the fourth leading cause of cancer-related deaths.[1] It is projected that by 2025, over one million people will be diagnosed with liver cancer each year.[2,3] China has a high incidence of liver cancer, with its mortality rate rising from third place in 2018 to second place in 2020,[4,5] which undoubtedly imposes a heavy economic burden on society. Currently, treatment options for liver cancer include surgical resection, chemotherapy, immunotherapy, targeted therapy, and interventional therapy.[2,6,7] However, the five-year recurrence rate remains as high as 70% even after surgical resection.[2,8–10] Immune escape, targeted resistance, and relapse are primary causes of treatment failure in liver cancer patients.[11]

Received: 10 September 2024
Accepted: 12 November 2024
Published: 18 November 2024

The TME plays a crucial role in the development of cancers, including tumor cells, immune cells, blood vessels, and extracellular matrix (ECM). CAFs and tumor-associated macrophages(TAMs) are the two major components of the TME and play essential roles in tumor initiation and progression.[12,13] Studies on CAFs have revealed their role in promoting tumor progression. However, the mechanisms by which CAFs regulate liver cancer are not fully understood. Lin et al found in an scRNA-seq analysis that pleiotrophin (PTN) secreted by hepatocellular carcinoma-associated fibroblasts (H-CAFs) mediates the progression from chronic viral hepatitis B and cirrhosis to HCC.[14] In our study, we used R (Version 4.4.1) to analyze the scRNA-seq datasets of healthy human liver tissue (GSE158723) and liver cancer tissue (GSE112271) obtained from the National Center for Biotechnology Information (NCBI) Gene Expression Omnibus (GEO, https://www.ncbi.nlm.nih.gov/geo/query/acc.cgi) database. In addition, CAFs may influence HCC progression through PTN/SDC2 signaling. Furthermore, CAFs derived pleiotrophin may enhance the interaction between CAFs and HCC cells by binding to the syndecan-2 (SDC2) receptor; suggesting that PTN may serve as a new biomarker for the early diagnosis of HCC and may provide new therapeutic strategies.

Methods and Materials

Analysis of scRNA-seq Datasets

Download scRNA-seq datasets (GSE158723 and GSE112271) from NCBI GEO. The dataset GSE158723 included two liver samples. The first liver sample has two samples from the parenchymal fraction and two samples from the non-parenchymal fraction; the second liver sample has one sample from the parenchymal fraction, two samples from the non-parenchymal fraction, and one sample from the whole fraction. Dataset GSE112271 consisted of three and four tumor samples from two different individuals. We filtered cells from the GSE158723 dataset, retaining those with unique feature counts between 200 and 4,500 and mitochondrial counts exceeding 25%; For the GSE112271 dataset, the filtering criteria were unique feature counts between 200 and 6,000 and mitochondrial counts exceeding 30%; Genes detected in fewer than 3 cells were labelled as undetected.

Clinical Liver Cancer Tissue Collections and Assays

Liver cancer tissues and paired adjacent tissues from patients with HCC who underwent surgical resection and did not receive any anti-tumor therapy before in The Department of Hepatobiliary Surgery, Affiliated Hospital of Youjiang Medical University for Nationalities were collected for frozen section preparation (6μm, 8μm, and 20μm) and single-cell suspension preparation (Figure 1A). The single-cell suspension was stained with the following antibodies: Vimentin-PerCP-y5.5 (Santa Cruz Biotechnology, #sc-6260), PTN-AF488 (Santa Cruz Biotechnology, #SC-74443), AFP-PE (SinoBiological, #12177-MM35-P), and SDC2-A647 (Santa Cruz Biotechnology, #sc-365624), and analyzed by flow cytometer (Life Technologies Holdings pte, #Attune NxT). FlowJo software (version 10.6.2) was used to analyze the data. The 8μm frozen sections were stained with Masson (Shanghai Biyuntian Biotechnology Co., Ltd., #L20J12G138259). The 6μm and 20μm frozen sections were underwent to immunofluorescence staining using the following antibodies: PTN-AF488 (Santa, #SC-74443), vimentin (Invitrogen, #MA5-16409), AFP (Invitrogen, #14-9760-82), SDC2 (Invitrogen, #36-6200), and DAPI (Invitrogen, #62248). Images were captured using a binocular stereo microscope (Leica Microsystems Shanghai Trade Co., LTD., #EZ4W) and laser scanning confocal microscope (ZEISS, #LSM 980), respectively. ImageJ software was used to process and analyze the images, and GraphPad Prism 9.5.1 software was used for statistical analysis.

Single Cell Preparation

The clinically collected liver cancer tissue samples were chopped in a culture dish, and then moved to a 15mL centrifuge tube with Hank's Balanced Salt Solution to 6mL, then added to collagenase IV 6ul, and then placed in a water bath at 37° C for 10 min, and then taken out to observe the cell degradation, repeat for 3 to 4 times.Finally, the digestion was terminated in the water bath with the same amount of PBS/0.5%BSA/2MMEDTA for 10 minutes, and then the single-cell suspension was filtered out with a 100-pore filter into a 50mL centrifuge tube for subsequent flow analysis.

Immunofluorescence Staining

The collected clinical liver cancer samples were made into frozen sections (6um, 8um and 20um), dried at room temperature for 15 min, fixed with anhydrous methanol at −20°C for 10 minutes, washed 3 times with 1X PBS for 5 min/ time, and then circle the samples with LIQUID BLOCKER pen after completely drying. With an Anti-Rh Fc Receptor Binding(Invitrogen): PBS/1%BSA=100:1 closed for 40 minutes, added the diluted primary antibody to the sample overnight at 4°C and incubated away from light according to manufacturer's instructions, washed 3 times with 1X PBS for 5 min/ time, added the diluted secondary antibody to the sample at room temperature and incubated away from light for 1 hour according to the manufacturer's instructions, washed 3 times with 1X PBS for 5 min/ time. According to the manufacturer's instructions, the diluted DAPI was added to the sample and incubated at room temperature in the dark for 5 minutes, washed 3 times with 1X PBS for 5 min/ time, sealed with anti-fluorescein quencher and covered with cover glass.

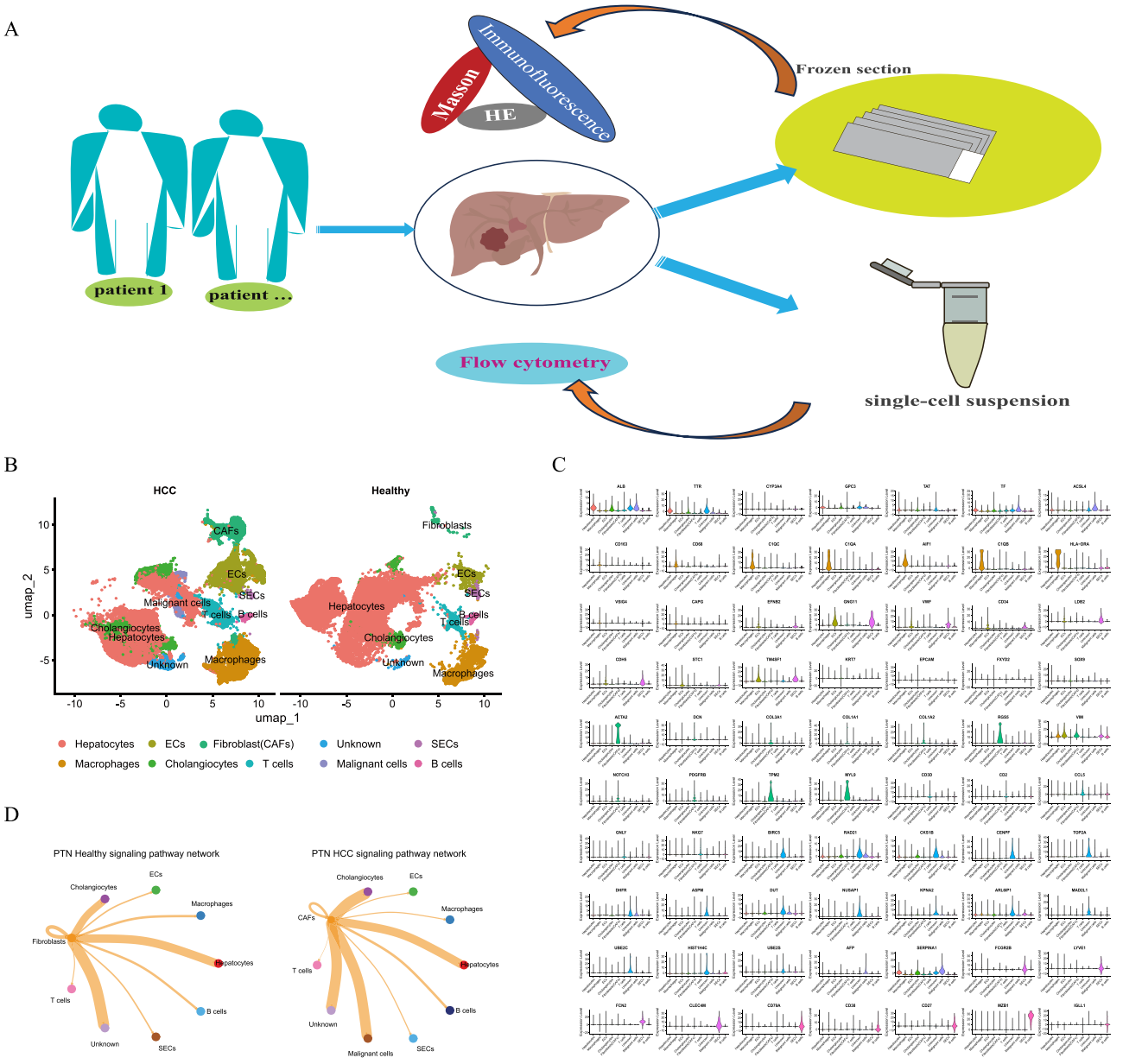

Figure 1 Continued.

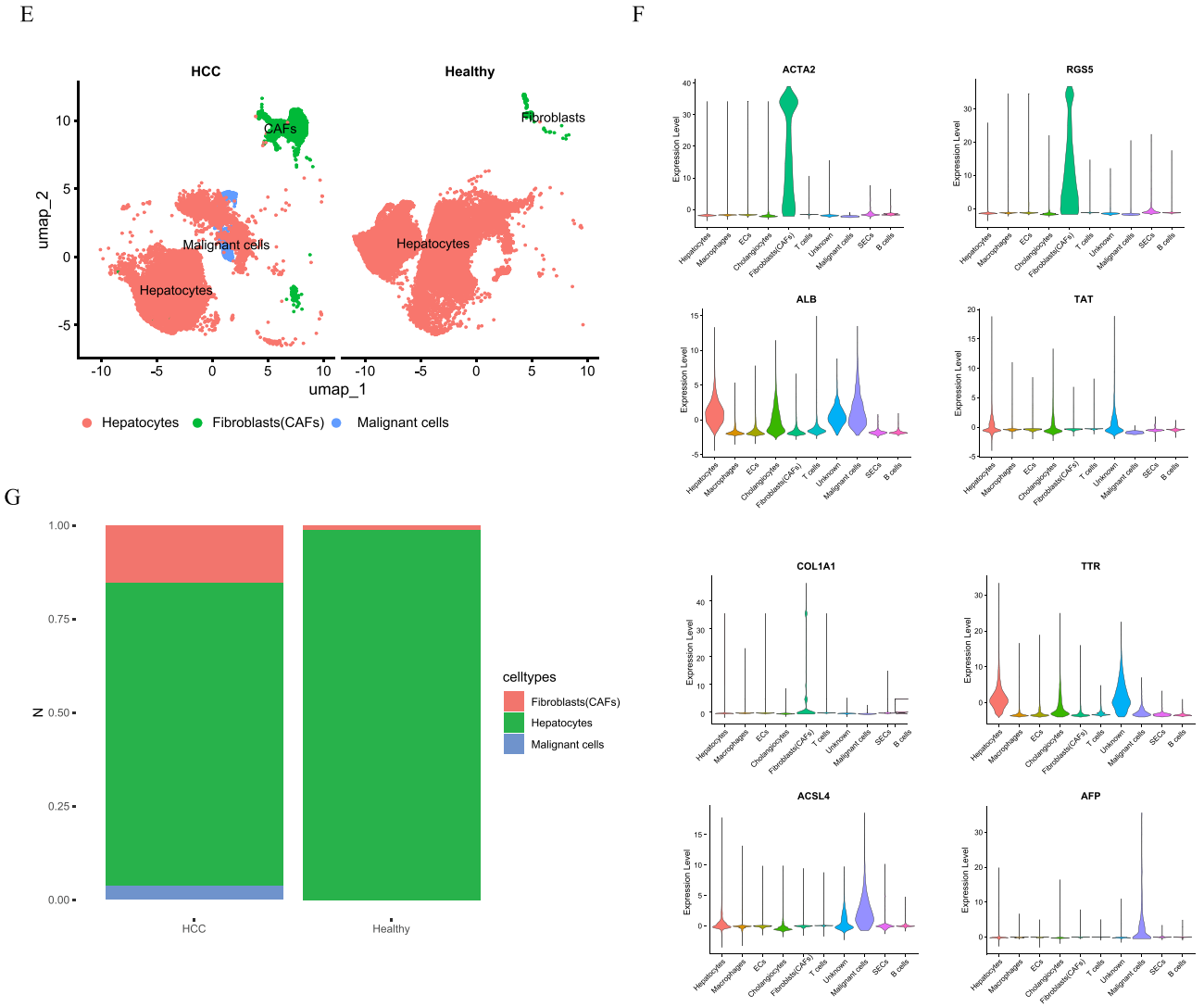

Figure 1 Proportion of CAFs in HCC and Healthy Groups. (**A**) Flowchart of clinical sample experiments. (**B**) Cell types annotated in healthy and HCC groups, with an increase in some cell types in HCC. (**C**) Markers for all annotated cell types. (**D**) Comparison of fibroblasts (CAFs) interactions with other cells via PTN signaling pathway. (**E**) Fibroblasts (CAFs), hepatocytes and malignant cells were extracted for visualization and comparison. (**F**) Markers for various cell types, indicating changes in cell populations between healthy and HCC groups. (**G**) The proportion of fibroblasts, hepatocytes and malignant cells in healthy and HCC group was visualized as a stacked bar graph.

Cell Culture and Assays

Lo2 (Aorisai Biotechnology (Shanghai) Co., LTD, product number: ORC0427) and Huh-7 (Aorisai Biotechnology (Shanghai) Co., LTD, product number: ORC0100) cell lines were cultured (The cell density and growth status of the received cells were observed under the microscope. When the cell density reached about 90%, the medium was discarded, and 1mL 0.25% pancreatic enzyme was added after washing with PBS twice for digestion at 37°C for about 3 minutes. After the cells became round under the microscope, 2mL DMEM medium containing 10% fetal bovine serum and 1% penicillin-streptomycin was added to terminate the digestion. After gently dispersing the cells, the cells were transferred into a 15mL centrifuge tube, centrifuged at 1000 RPM for 3 minutes, and after the medium was discarded, 10mL DMEM medium containing 10% fetal bovine serum and 1% penicillin-streptomycin was added to re-suspend the cells, and the cells were passed into a T25 culture bottle at 1:2 and cultured in a 5%CO_2 incubator at 37°C) and made into cell slides, and immunofluorescence staining was performed using antibodies SDC2 (Invitrogen, #36-6200), DAPI (Invitrogen, #62248).

Statistical Analysis

All statistical analyses were performed using GraphPad Prism 9 (GraphPad Software, San Diego, CA, USA). For normally distributed data, continuous variables are expressed as mean ± standard deviation (SD). For non-normally distributed data, the Shapiro–Wilk test is used to evaluate the normality of the data. For comparison between the two groups, unpaired Student's *T*-tests were used for the normally distributed data. All statistical tests were two-tailed, and a p-value of less than 0.05 was considered statistically significant. The confidence interval (CI) was set at 95%, P<0.05 was considered to indicate a statistically significant difference.

Results

The Single Cell Atlas of Human Healthy Liver and Hepatocellular Carcinoma

Using R language analysis software, we performed quality control and removed mitochondrial genes from the datasets (GSE158723 and GSE112271) using the PercentageFeatureSet R package. This ensured that each of the 27,205 cells in the GSE158723 dataset expressed between 200 and 4,500 genes, with less than 25% being mitochondrial genes.[15] Similarly, for the GSE112271 dataset, each of the 38,017 cells expressed between 200 and 6,000 genes, with less than 30% being mitochondrial genes[16] (Supplementary Figure 1A and B). We then merged the two datasets and normalized them using the logarithmic method. Dimensionality reduction and clustering were performed using Seurat R package at a resolution of 0.5 with the Seurat R package. The AnnotationHub R package was used to annotate the cell populations after clustering, in combination with published literature and cell marker databases (CellMarker 2.0, CellMarker (xbio.top)), and to visualize the results with a Uniform Manifold Approximation and Projection (UMAP) diagram (Figure 1B). Hepatocytes were marked by ALB, TTR, CYP3A4, GPC3, TAT, TF, and ACSL4; macrophages (Kupffer cells) were marked by CD163, CD68, C1QC, and C1QA; endothelial cells (ECs) were marked by EFNB2, GNG11, VWF, CD34, LDB2, and CDH5; cholangiocytes were marked by KRT7, EPCAM, FXYD, and SOX9; fibroblasts and CAFs were marked by ACTA2, DCN, COL3A1, COL1A1, COL1A2, RGS5, VIM, NOTCH3, PDGFRB, TPM2, and MYL; T cells were marked by CD3D, CD2, CCL5, GNLY, and NKG7; malignant cells were marked by AFP, ACSL4, and SERPINA1; sinusoidal endothelial cells (SECs) were marked by FCGR2B, LYVE1, FCN2, and CLEC4M; and B cells were marked by CD79A, CD38, CD27, MZB1, and IGLL1.[15,17–19] Notably, a group of clusters expressed BIRC5, CENPF, TOP2A, DHFR, ASPM, NUSAP1, KPNA2, MAD2L1, and UBE2C (Figure 1C). Using the CellChat R package to analyze and visualize the communication network weights and signaling pathways between the two scRNA-seq datasets, we found that fibroblasts (CAFs), ECs, T cells, macrophages, and unknown populations were increased in HCC, whereas CAFs showed a significant increase and hepatocytes showed a significant decrease compared to those in the healthy group (Figure 1B). Protein-protein interaction (PPI) and ligand-receptor pair analysis using CellChat R package indicated that CAFs and HCC cells may regulate the occurrence and development of liver cancer via PTN signaling pathway; in PTN signaling pathway, CAFs had the strongest interactions with cholangiocytes, SECs, hepatocytes, malignant cells, and unknown cell populations (Figure 1D). Based on literature and relevant materials, these clusters could not be identified at this time and were annotated as "Unknown". Upon comparison, it was found that the proportion of this cluster in the HCC group was significantly higher than that in the healthy group (Figure 1B), although the unknown cell population has not been identified, the results from the CellChat R package analysis suggested it may play an important role in normal liver function and in the progression of liver cancer, it may be the basic cell population to maintain liver function.

The Proportion of CAFs in Human Hepatocellular Carcinoma

To further explore the important role of CAFs in the occurrence and development of HCC, fibroblasts (CAFs), hepatocytes, and malignant cells were extracted separately and visualized as UMAP (Figure 1E). ACTA2, COL1A1, DCN, and RGS5 were used to mark fibroblasts (CAFs). Currently, no single gene is used to mark fibroblasts (CAFs) and researchers commonly use a combination of markers such as ACTA2, COL1A1, and Vimentin.[14,20] The hepatocytes were marked by ALB, TAT, and TTR, whereas the malignant cells were marked by ACSL4 and AFP (Figure 1F). Analysis of the scRNA-seq datasets (GSE158723 and GSE112271) demonstrated that the proportion of fibroblasts (CAFs) was higher in HCC tissues than that in healthy livers. A comparison of extracted fibroblasts (CAFs) and hepatocytes in a stacked bar chart showed a significant increase in the HCC

group compared to that in the healthy group (Figure 1G). As a key component of the TME, CAFs may significantly influence HCC progression.[12,21,22] We then performed flow cytometry and immunofluorescence staining for clinical liver cancer and adjacent tissues (Figure 1A). Flow cytometry analysis showed that AFP expression is higher in HCC tissues than in the adjacent tissues (Figure 2A). As the most commonly used clinical diagnostic marker of HCC, higher levels of AFP are associated with worse clinical prognoses[23,24] Many patients with HCC are diagnosed at an advanced stage with a high level of AFP in their peripheral blood,[25] so it is necessary to find a novel biomarker for early HCC diagnosis. Multiple immunofluorescent staining and confocal laser microscopy images showed that CAFs constituted a greater proportion in tumor tissues compared to adjacent tissues, which most CAFs in tumor tissues distributed in cords surrounding tumor cells; CAFs were mainly distributed in vascular areas, showing a scattered distribution outside these areas in adjacent tissue; the proportion difference of CAFs between cancer and adjacent groups was statistically significant ($p < 0.05$) (Figure 2B). Flow cytometry analysis revealed that the proportion of CAFs in cancer tissues was significantly higher than in adjacent tissues, with a statistically significant difference ($p < 0.05$) (Figure 2C), consistent with the scRNA-seq data analysis. Masson's staining corroborated these findings, indicating a higher degree of fibrosis in tumor tissues than in adjacent tissues. In adjacent tissues, fibrosis was primarily located in vascular regions composed mainly of fibrocytes, whereas other areas exhibited sporadic punctate fibrosis. In tumor tissues, fibrosis was primarily distributed in the cords surrounding tumor cells (Figure 2D). Gene

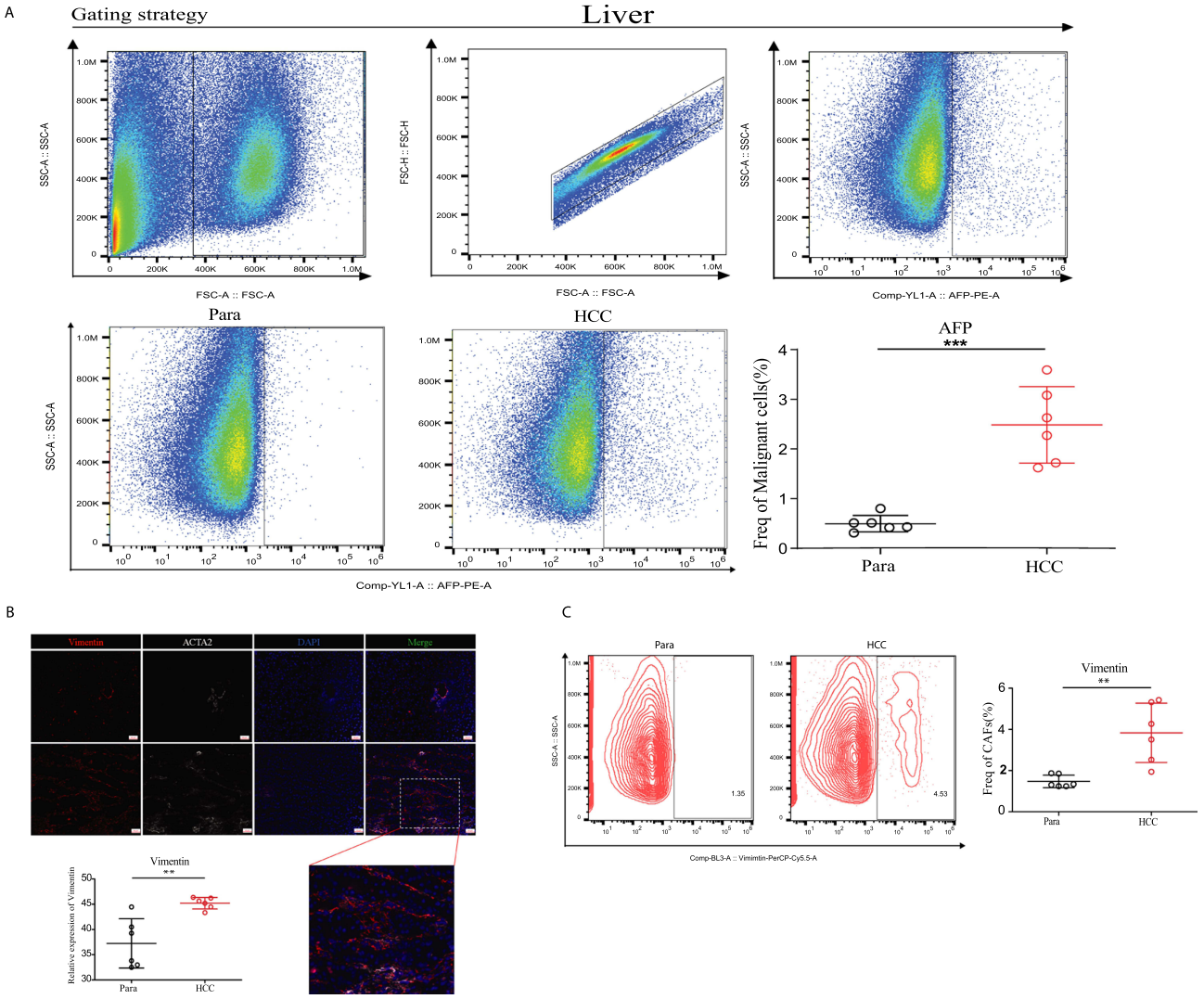

Figure 2 Continued.

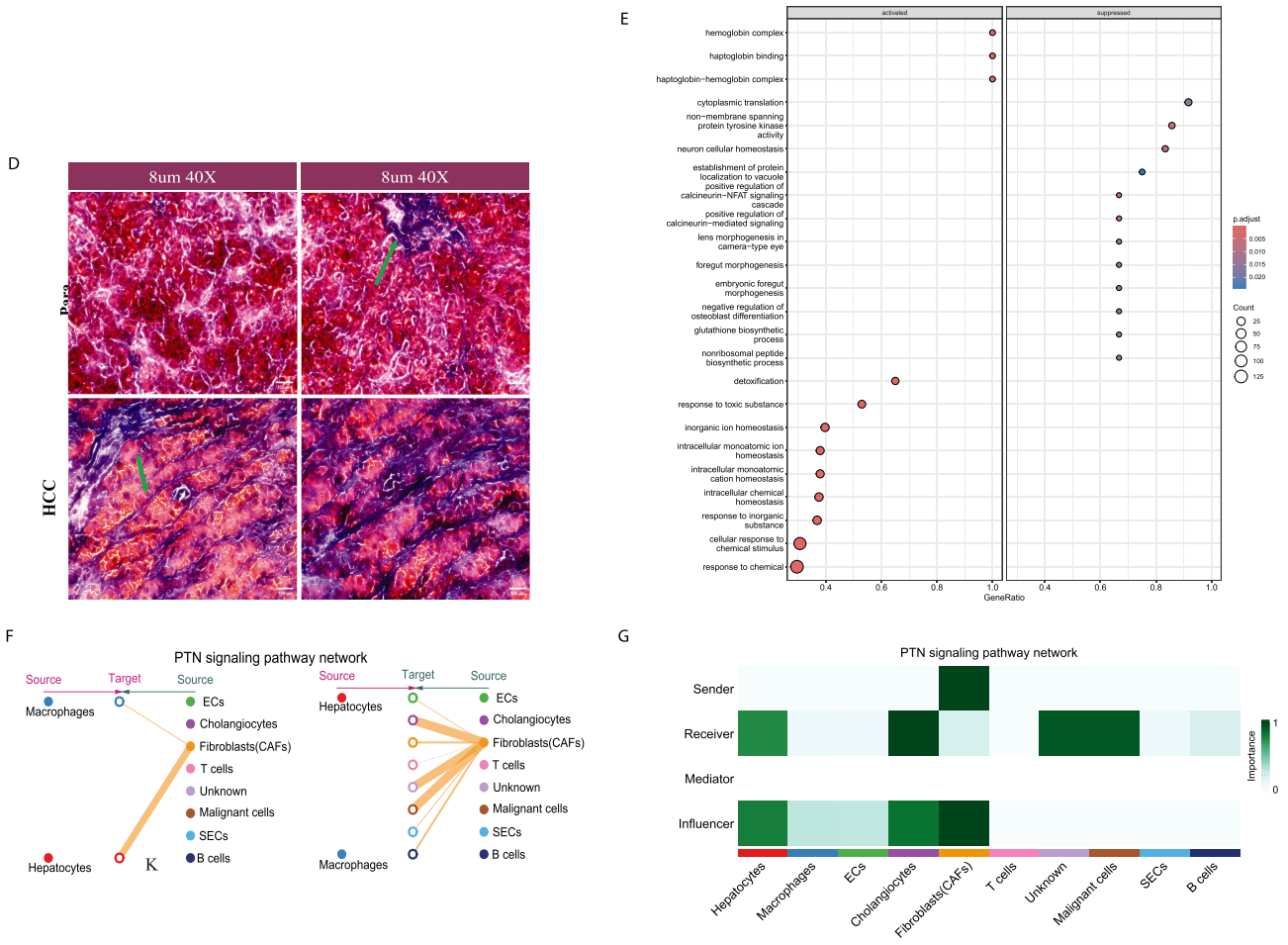

Figure 2 Proportion of CAFs in Liver Cancer Tissues. (**A**) Flow cytometry analysis showing higher AFP expression in cancer tissues. (**B**) Immunofluorescence experiments revealing higher CAFs proportions in cancer tissues and distribution around cancer cells. (**C**) Flow cytometry analysis showing higher CAFs proportions in cancer tissues. (**D**) Masson staining indicating increased fibrosis in cancer tissues, as indicated by the green arrow. (**E**) Gene enrichment analysis highlighting CAF roles. (**F**) PPI and ligand-receptor analysis indicating CAFs' regulatory role in liver cancer. (**G**) Heat map analysis of PTN signaling pathway interactions. ***: P<0.001, **: P<0.01, P<0.05: the difference was statistically significant. Green arrow: the green arrow indicates the site of fibrosis.

enrichment analysis (GEA) of fibroblasts (CAFs) indicated that they mainly play roles in intracellular ion and chemical homeostasis, responding to chemical stimuli, synthesizing hemoglobin, and inhibiting non-transmembrane protein tyrosine kinase activity (Figure 2E). This may explain the significant role of CAFs in liver tissues and their mechanism of resisting to tyrosine kinase inhibitors (TKIs).

The Mechanism of PTN Signaling Pathway in Human Hepatocellular Carcinoma

Given that scRNA-seq data analysis indicated a significant increase in CAFs in HCC compared to the healthy group, we validated their expression through clinical liver cancer tissue and adjacent tissue assays. However, the specific mechanism through which CAFs promote HCC progression remains unclear. A scRNA-seq analysis by Lin et al found that PTN derived from CAFs may bind to receptors (such as NCL, SDC1, and SDC2) on hepatocytes or malignant cells, mediating the progression from chronic viral hepatitis B to cirrhosis to HCC.[14] Analyzing the scRNA-seq datasets (GSE158723 and GSE112271), we found that CAFs mediate interactions with hepatocytes, hepatoma cells, and cholangiocytes through the PTN signaling pathway; ligand-receptor pair analysis using the CellChat R package showed that signals sent by CAFs are primarily received by hepatocytes, cholangiocytes, unknown, and malignant cells, indicating strong interactions between CAFs and these cells (Figure 2F and G). The analysis revealed that PTN secreted by fibroblasts in healthy tissues mainly binds to SDC1, SDC2, SDC3, SDC4, NCL, and ALK receptors on hepatocytes and cholangiocytes, with the PTN-SDC4

ligand-receptor pair contributing the most; PTN primarily binds to SDC1, SDC2, SDC4, and NCL receptors on hepatocytes, cholangiocytes, and malignant cells, with the PTN-SDC2 ligand-receptor pair being the most significant contributor in the HCC group, and we sketched out the general mechanism (Figure 3A and B), similar to the findings by Lin et al[14,26] Through scRNA-seq data analysis, we found that PTN is mainly derived from fibroblasts (CAFs) in both normal liver and HCC tissues, with its signals primarily received by the corresponding receptors on hepatocytes, cholangiocytes, and cancer cells (Figure 3C–E).

We further calculated the interaction strength of the PTN-SDC2 ligand-receptor pair and compared the differences between the healthy and HCC groups. In the healthy group, the PTN-SDC2 ligand-receptor pair mainly facilitated interactions between fibroblasts and hepatocytes and the unknown cell group, with weaker interactions with cholangiocytes, whereas in the HCC group, the PTN-SDC2 ligand-receptor pair exhibited stronger interactions between fibroblasts and hepatocytes, cancer cells, cholangiocytes, and the unknown cell group, indicating stronger interactions compared to the healthy group (Figure 3F and G).

Comparative analysis of the scRNA-seq datasets (GSE158723 and GES112271) revealed that PTN expression is higher in the HCC group than in the healthy group (Figure 3H). The information flow of the PTN signaling pathway was visualized in a stacked bar chart, indicating a stronger information flow of PTN signals in the HCC group than in the healthy group (Figure 4A). Thus, we speculate that PTN is upregulated in HCC and may promote HCC progression. Multiple immunofluorescence staining of clinical HCC samples showed increased PTN expression in cancer tissues compared to adjacent tissues, with a statistically significant difference ($p < 0.05$) (Figure 4B). Confocal laser microscopy imaging indicated that fibroblast-derived PTN are primarily distributed among tumor cells and may migrate to tumor cells after secretion, bind to receptors on tumor cells, and regulate their activity (Figure 4B). Additionally, single-cell suspensions of clinical HCC samples were analyzed using flow cytometry. PTN expression was significantly higher in cancer tissues than that in adjacent tissues ($p < 0.05$), with a statistically significant difference (Figure 4C and D).

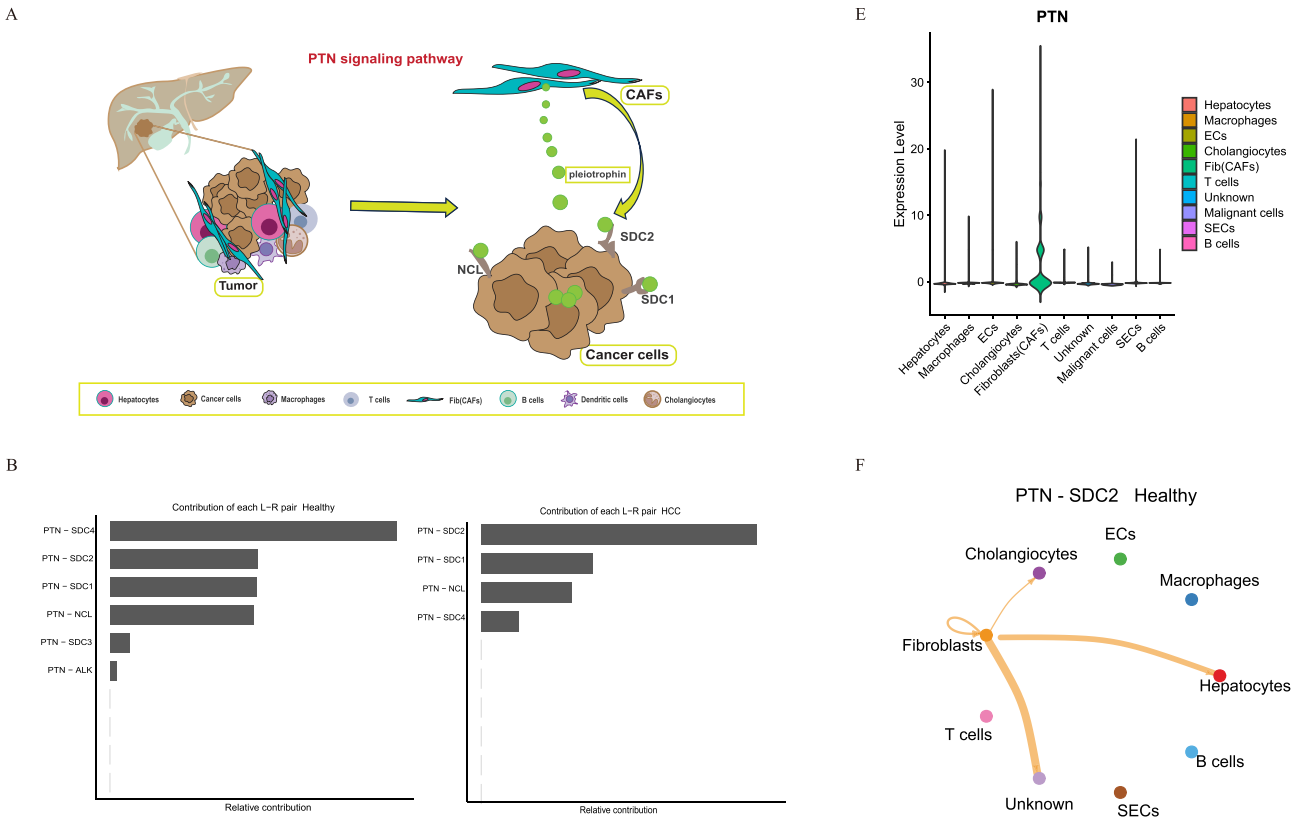

Figure 3 Continud.

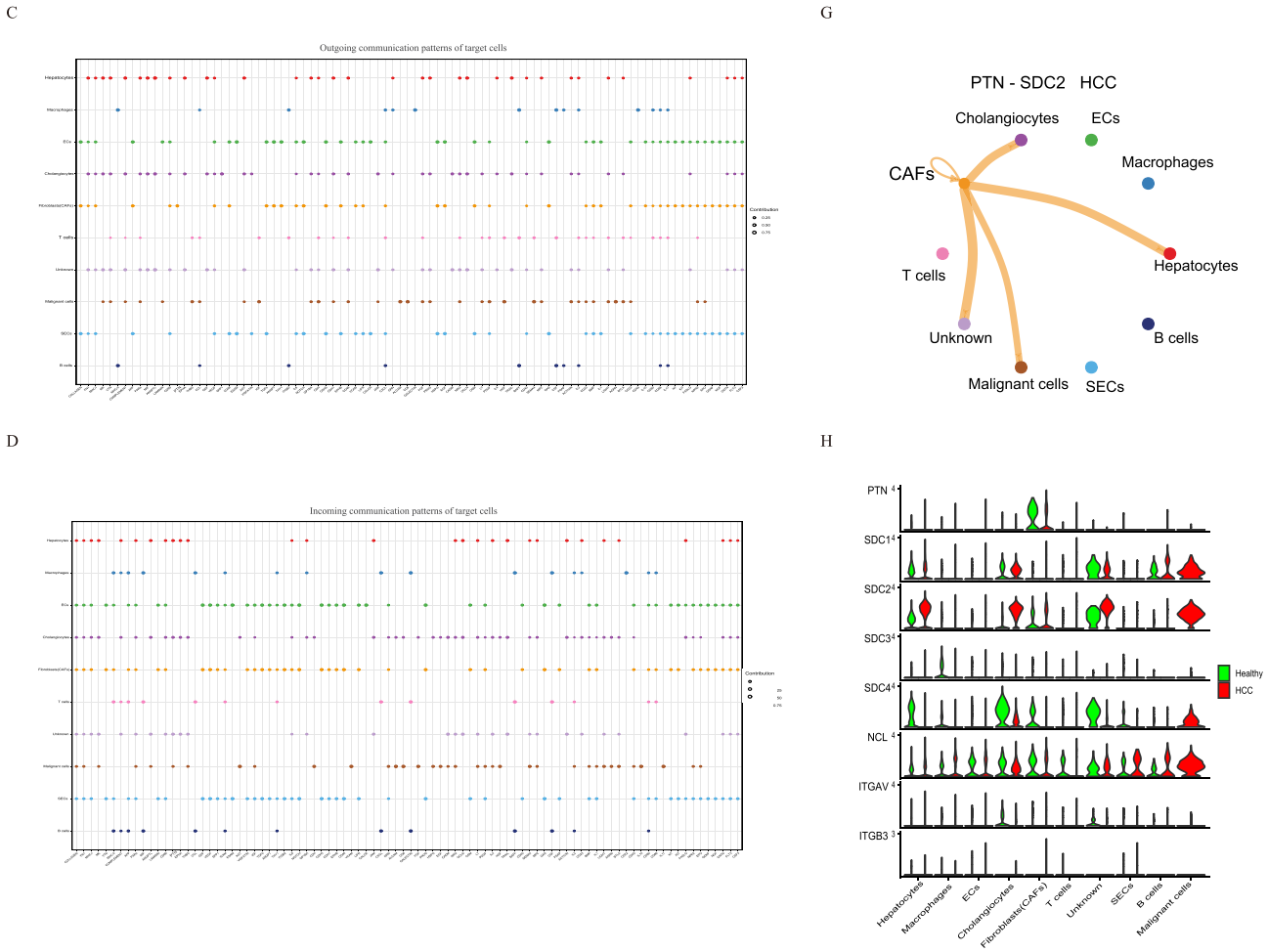

Figure 3 Mechanism of PTN Signaling Pathway in HCC. (**A**) Molecular mechanism diagram of the PTN pathway. (**B**) Ligand-receptor pair analysis showing different contributions in healthy vs HCC groups. (**C**–**E**) Pleiotrophin secretion by CAFs and its receptors. (**F** and **G**) Interaction patterns of PTN-SDC2 in healthy vs HCC groups. (**H**) Higher PTN expression in HCC vs healthy groups.

The Expression of SDC2 in HCC Samples and Cell Lines

According to scRNA-seq analysis, CAFs derived PTN enhances the interaction between CAFs and HCC cells by binding to SDC2 receptor on HCC cells; but the mechanism of which CAFs modulate HCC cells is unclearly, then we hypothesize that CAFs may regulated HCC via PTN/SDC2 signaling. We performed immunofluorescent staining on Lo2 and Huh-7 cell lines, found that the SDC2 expression in Huh-7 cell line is higher than in Lo2 cell line, the difference was statistically significant with $p<0.05$ (Figure 4E and F). Flow cytometry analysis of clinical HCC samples showed the same results; the SDC2 expression in cancer tissues was significantly higher than that in adjacent tissues ($p<0.05$) (Figure 4G and H).

Discussion

The pathological types of primary liver cancer include hepatocellular carcinoma, intrahepatic cholangiocarcinoma (iCCA), and mixed-cell carcinoma.[27] Most patients with liver cancer are chronic hepatitis B virus carriers,[28] and HCC often evolves along the chronic hepatitis B virus-cirrhosis-HCC axis.[29] scRNA-seq analysis of datasets (GSE158723 and GSE112271) shown a decreasing trend of hepatocytes in HCC, and flow cytometry analysis of clinical HCC samples showed that adjacent tissues also secrete a small amount of AFP because of the complexity and heterogeneity of cancers, and adjacent tissues may possess certain tumor characteristics and phenotypes

during tumor progression. We performed scRNA-seq analysis, which suggested that CAFs accounted for an increased proportion of HCC cases, and flow cytometry and immunofluorescence staining of clinical HCC samples validated these results. CAFs are among the most abundant stromal cells in HCC, producing substantial amounts of collagen, leading to fibrosis and promoting HCC development.[14,22,30] We speculated that fibroblasts in adjacent tissues are also abnormal and may possess tumor-promoting properties, potentially defining them as pre-CAFs. CAFs contribute to HCC progression via various pathways. Jia et al showed that CAFs in HCC induce epithelial-mesenchymal transformation (EMT) via the IL6/IL6R/STAT3 axis and confirmed that the interactions between CAFs and HCC cells promote a favorable TME.[22] CAFs derived Secreted Phosphoprotein-1 (SPP1) enhances TKI resistance in HCC through gene signaling bypass activation of EMT, with increased SPP1 expression closely related to tumor evolution and microenvironment reprogramming.[31,32] Functional enrichment analysis of CAFs showed similar results. Liu et al found that fibroblast-derived C-X-C motif chemokine ligand 11 (CXCL11) enhanced HCC progression and metastasis by activating chemotaxis and T-cells in tumor cells.[21] Our scRNA-seq analysis indicated that CAFs have the strongest interactions with hepatocytes, HCC cells, and cholangiocytes, suggesting that CAFs may play a crucial role in HCC development. These findings suggest that targeting the TME may be a novel strategy for HCC treatment.[33] PTN play vital roles in growth, survival, differentiation, and tumorigenesis.[34] It has been implicated in the occurrence and development of several tumors, including glioblastoma, prostate cancer, and epithelial ovarian cancer.[35–38] PTN mediates its tumor-promoting effects through various signaling pathways, including IRE-1, AKT, ERK, STAT3, and WNT.[39] Sehi et al provided experimental evidence that PTN and its signaling components are significant in the pathogenesis of epithelial ovarian cancer,

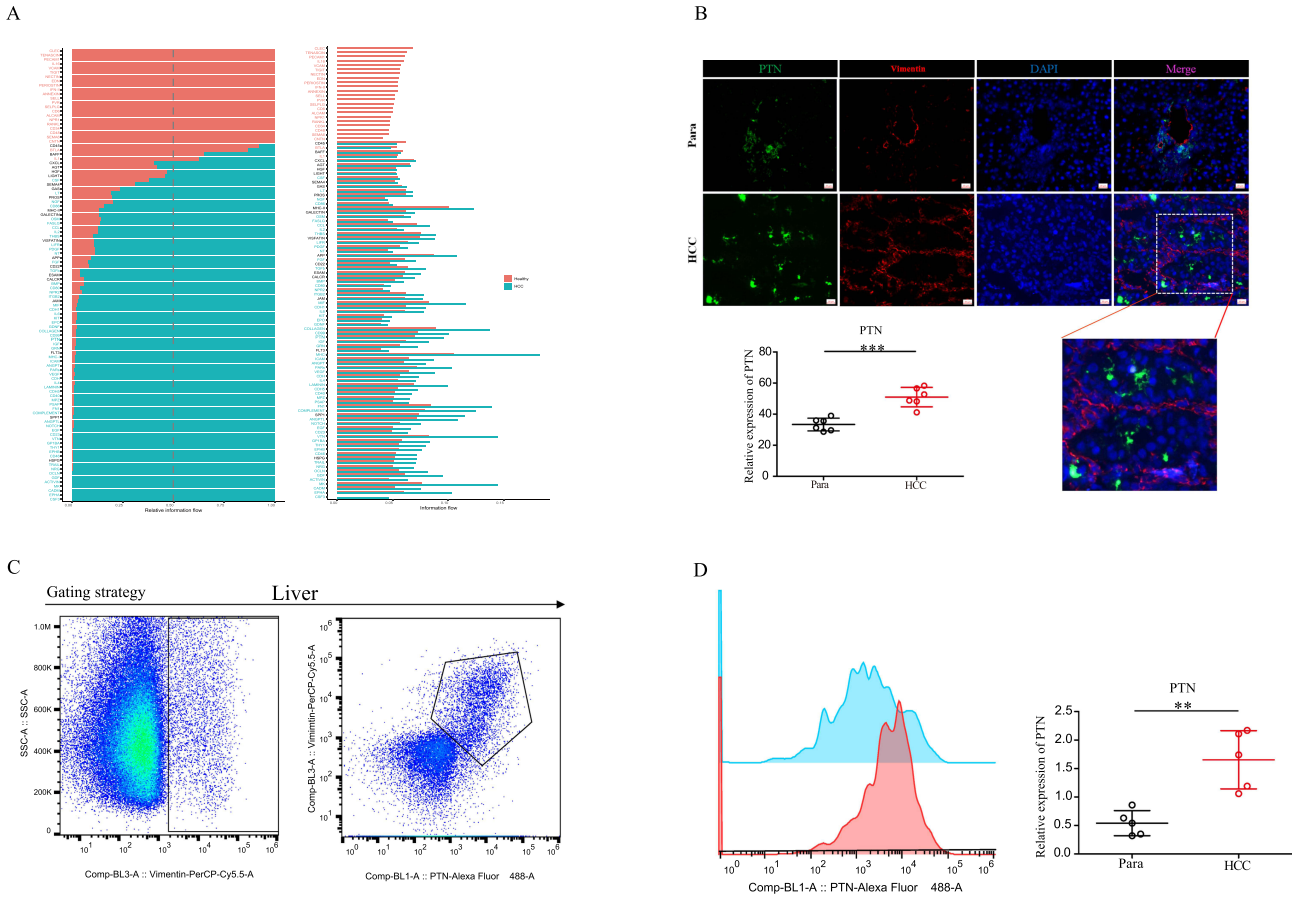

Figure 4 Continued.

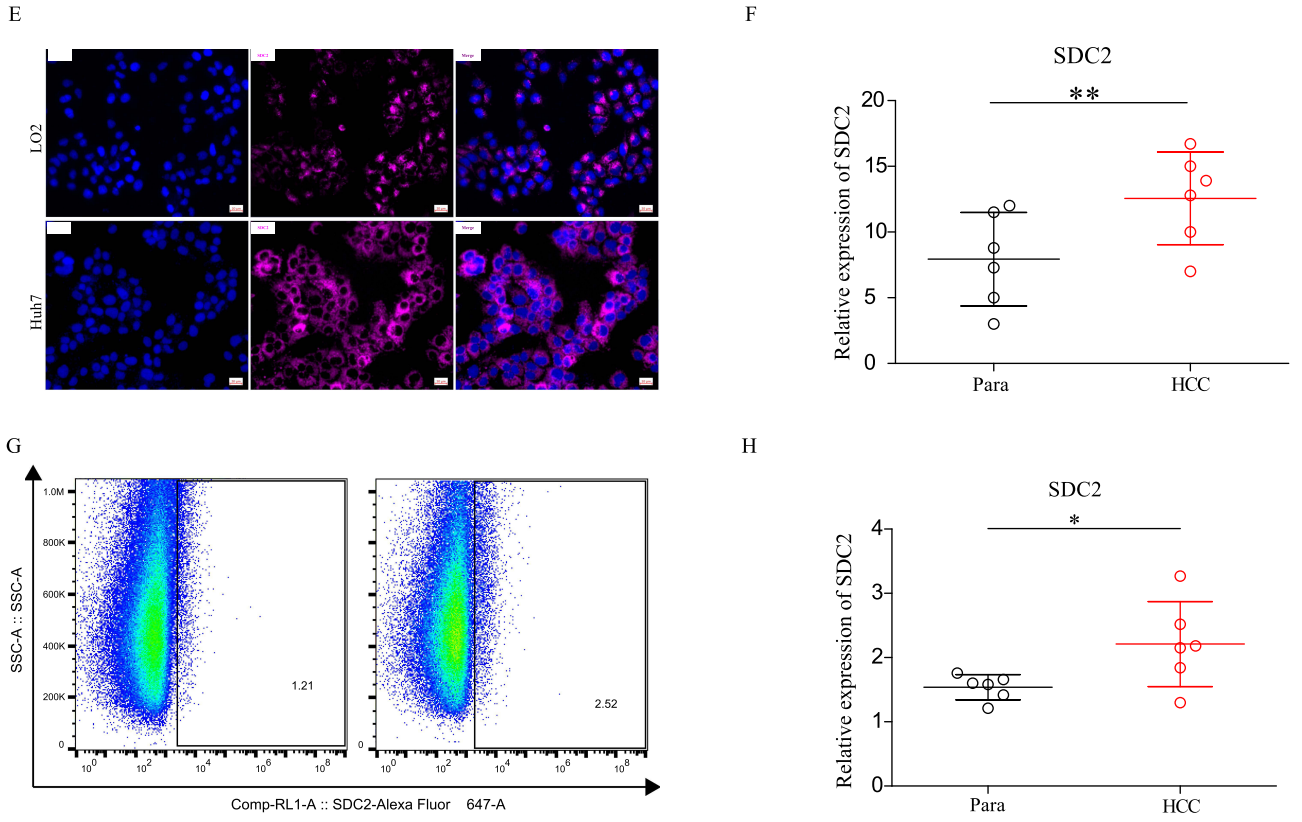

Figure 4 PTN Expression in HCC and SDC2 Expression of Cell Lines. (**A**) Visualization of PTN signaling information flow. (**B**) Confirmation of higher PTN expression in cancer tissues through immunofluorescence and imaging. (**C** and **D**) Flow cytometry analysis confirming PTN expression differences between cancer and adjacent tissues. (**E** and **F**) The expression of SDC2 in Huh-7 cell line vs Lo2 cell line. (**G** and **H**) Flow cytometry analysis confirming SDC2 expression differences between cancer and adjacent tissues. ***: P<0.001, **: P<0.01, *: P<0.05, P<0.05: the difference was statistically significant.

providing a theoretical basis for the clinical evaluation of MAPK inhibitors in ovarian tumors expressing PTN and/or PTPRZ1.[35] However, the role of PTN in HCC remains unclear. Our study suggests that PTN expression is higher in HCC, and that PTN is secreted by CAFs. After secretion, it combines with the receptors (SDC2, SDC1, NCL, and SDC4) to promote tumor progression. In our experiments, SDC2 exhibited higher expression in HCC and may play an important role in HCC progression. PTN levels are higher in HCC tissues than in adjacent and normal liver tissues, and a meta-analysis identified PTN as a promising biomarker, suggesting that targeting PTN may represent a novel clinical treatment strategy.[40–42]

Conclusion

In our study, using scRNA-seq dataset analysis, we uncovered the principal constituents of the TME in liver cancer and delineated their contribution to HCC progression. Experimental validation confirmed that CAFs are more abundant in tumor tissues than in adjacent tissues. Notably, the expression levels of PTN and SDC2 are significantly elevated in HCC. Through cell interaction and PPI network analysis, we discovered significant crosstalk between CAFs and HCC cells, mediated by PTN/SDC2 signaling, suggesting that therapeutic targeting of CAFs could offer a novel and promising therapeutic approach for HCC. Furthermore, PTN's enhanced expression profile of PTN is a potential novel biomarker for HCC diagnosis, warranting further investigation of its clinical utility.

Data Sharing Statement

Data and materials are provided along with the manuscript.

Ethics Approval and Consent to Participate

Our study complies with the Declaration of Helsinki to ensure ethical standards are met in the conduct of research involving human participants. And all the participants have been informed all the information about this study and signed the informed consent. This study was approved by the Ethics Committee of the Affiliated Hospital of Youjiang Medical University for Nationalities [#YYFY-LL-2022-55(8)].

Author Contributions

All authors have substantially contributed to this work, whether in the areas of conceptualization, study design, implementation, data acquisition, analysis, or interpretation. They also participated in drafting, revising, or critically reviewing the manuscript, provided final approval for the version to be published, consented to the journal selection for submission, and take responsibility for all aspects of the work. Wenxian Lin, Lizhu Tang and Chenyi Zhuo contributed equally to this study.

Funding

This work was supported by the National Natural Science Foundation of China (#82160589), Guangxi Science and Technology Major Project (#GuikeAA23073013), The Natural Science Foundation of Guangxi Zhuang Autonomous Region (#2024GXNSFAA010126), Nanning Qingxiu District Science and Technology Bureau Key Research and Development Plan (#2020035), Guangxi Key Laboratory of Early Prevention and Treatment for Regional High-Frequency Tumors (#GXK201604), Key Laboratory of Basic Research on Regional Diseases (Guangxi Medical University), Education Department of Guangxi Zhuang Autonomous Region (#GXQYJB2023001), and Guangxi Medical and Health Program for Promotion (#s2022140).

Disclosure

The authors declare that this research was conducted in the absence of any commercial or financial relationships that could be construed as potential conflict of interest.

References

1. An LAN, Hongmei Z, Xianhui R, et al. Advances in epidemiology of hepatocellular carcinoma and intrahepatic cholangiocarcinoma. *Chin Tumor*. 2020;29(11):879–884.
2. Vogel A, Meyer T, Sapisochin G, Salem R, Saborowski A. Hepatocellular carcinoma. *Lancet*. 2022;400(10360):1345–1362. doi:10.1016/S0140-6736(22)01200-4
3. Louis DN, Perry A, Wesseling P, et al. The 2021 WHO classification of tumors of the central nervous system: a summary. *Neuro Oncol*. 2021;23(8):1231–1251. doi:10.1093/neuonc/noab106
4. Cao W, Chen HD, Yu YW, Li N, Chen WQ. Changing profiles of cancer burden worldwide and in China: a secondary analysis of the global cancer statistics 2020. *Chin Med J*. 2021;134(7):783–791. doi:10.1097/CM9.0000000000001474
5. Dong W, Xie Y, Huang H. Prognostic value of cancer-associated fibroblast-related gene signatures in hepatocellular carcinoma. *Front Endocrinol*. 2022;13:884777. doi:10.3389/fendo.2022.884777
6. Wang Y, Deng B. Hepatocellular carcinoma: molecular mechanism, targeted therapy, and biomarkers. *Cancer Metastasis Rev*. 2023;42(3):629–652. doi:10.1007/s10555-023-10084-4
7. Singal AG, Yarchoan M, Yopp A, Sapisochin G, Pinato DJ, Pillai A. Neoadjuvant and adjuvant systemic therapy in HCC: current status and the future. *Hepatol Commun*. 2024;8(6):e0430. doi:10.1097/HC9.0000000000000430
8. Liu Y, Deng M, Wang Y, Wang H, Li C, Wu H. Identification of differentially expressed genes and biological pathways in para-carcinoma tissues of HCC with different metastatic potentials. *Oncol Lett*. 2020;19(6):3799–3814. doi:10.3892/ol.2020.11493
9. Ye Y, Wang Y, Xu H, Yi F. Network meta-analysis of adjuvant treatments for patients with hepatocellular carcinoma after curative resection. *BMC Gastroenterol*. 2023;23(1):320. doi:10.1186/s12876-023-02955-5
10. Sung H, Ferlay J, Siegel RL, et al. Global cancer statistics 2020: GLOBOCAN estimates of incidence and mortality Worldwide for 36 cancers in 185 countries. *CA Cancer J Clin*. 2021;71(3):209–249. doi:10.3322/caac.21660
11. Yang X, Yang C, Zhang S, et al. Precision treatment in advanced hepatocellular carcinoma. *Cancer Cell*. 2024;42(2):180–197. doi:10.1016/j.ccell.2024.01.007
12. Chen S, Morine Y, Tokuda K, et al. Cancer-associated fibroblast-induced M2-polarized macrophages promote hepatocellular carcinoma progression via the plasminogen activator inhibitor-1 pathway. *Int J Oncol*. 2021;59(2):59. doi:10.3892/ijo.2021.5239
13. He H, Chen S, Fan Z, et al. Multi-dimensional single-cell characterization revealed suppressive immune microenvironment in AFP-positive hepatocellular carcinoma. *Cell Discov*. 2023;9(1):60. doi:10.1038/s41421-023-00563-x
14. Lin C, Chen Y, Zhang F, Zhu P, Yu L, Chen W. Single-cell RNA sequencing reveals the mediatory role of cancer-associated fibroblast PTN in hepatitis B virus cirrhosis-HCC progression. *Gut Pathog*. 2023;15(1):26. doi:10.1186/s13099-023-00554-z
15. Payen VL, Lavergne A, Alevra Sarika N, et al. Single-cell RNA sequencing of human liver reveals hepatic stellate cell heterogeneity. *JHEP Rep*. 2021;3(3):100278. doi:10.1016/j.jhepr.2021.100278

16. Losic B, Craig AJ, Villacorta-Martin C, et al. Intratumoral heterogeneity and clonal evolution in liver cancer. *Nat Commun*. 2020;11(1):291. doi:10.1038/s41467-019-14050-z
17. Yu L, Shen N, Shi Y, et al. Characterization of cancer-related fibroblasts (CAF) in hepatocellular carcinoma and construction of CAF-based risk signature based on single-cell RNA-seq and bulk RNA-seq data. *Front Immunol*. 2022;13:1009789. doi:10.3389/fimmu.2022.1009789
18. Hao X, Zheng Z, Liu H, et al. Inhibition of APOC1 promotes the transformation of M2 into M1 macrophages via the ferroptosis pathway and enhances anti-PD1 immunotherapy in hepatocellular carcinoma based on single-cell RNA sequencing. *Redox Biol*. 2022;56:102463. doi:10.1016/j.redox.2022.102463
19. Chi H, Zhao S, Yang J, et al. T-cell exhaustion signatures characterize the immune landscape and predict HCC prognosis via integrating single-cell RNA-seq and bulk RNA-sequencing. *Front Immunol*. 2023;14:1137025. doi:10.3389/fimmu.2023.1137025
20. Morén A, Bellomo C, Tsubakihara Y, et al. LXRα limits TGFβ-dependent hepatocellular carcinoma associated fibroblast differentiation. *Oncogenesis*. 2019;8(6):36. doi:10.1038/s41389-019-0140-4
21. Liu G, Sun J, Yang ZF, et al. Cancer-associated fibroblast-derived CXCL11 modulates hepatocellular carcinoma cell migration and tumor metastasis through the circUBAP2/miR-4756/IFIT1/3 axis. *Cell Death Dis*. 2021;12(3):260. doi:10.1038/s41419-021-03545-7
22. Jia C, Wang G, Wang T, et al. Cancer-associated Fibroblasts induce epithelial-mesenchymal transition via the Transglutaminase 2-dependent IL-6/IL6R/STAT3 axis in Hepatocellular Carcinoma. *Int J Biol Sci*. 2020;16(14):2542–2558. doi:10.7150/ijbs.45446
23. Norman JS, Li PJ, Kotwani P, Shui AM, Yao F, Mehta N. AFP-L3 and DCP strongly predict early hepatocellular carcinoma recurrence after liver transplantation. *J Hepatol*. 2023;79(6):1469–1477. doi:10.1016/j.jhep.2023.08.020
24. Hsu PY, Liang PC, Chang WT, et al. Artificial intelligence based on serum biomarkers predicts the efficacy of lenvatinib for unresectable hepatocellular carcinoma. *Am J Cancer Res*. 2022;12(12):5576–5588.
25. Hu X, Chen R, Wei Q, Xu X. The landscape of alpha fetoprotein in hepatocellular carcinoma: where are we. *Int J Biol Sci*. 2022;18(2):536–551. doi:10.7150/ijbs.64537
26. Zhou W, Zhang S, Cai Z, et al. A glycolysis-related gene pairs signature predicts prognosis in patients with hepatocellular carcinoma. *PeerJ*. 2020;8:e9944. doi:10.7717/peerj.9944
27. Sia D, Villanueva A, Friedman SL, Llovet JM. Liver cancer cell of origin, molecular class, and effects on patient prognosis. *Gastroenterology*. 2017;152(4):745–761. doi:10.1053/j.gastro.2016.11.048
28. Razavi-Shearer D, Gamkrelidze I, Pan C. Global prevalence, cascade of care, and prophylaxis coverage of hepatitis B in 2022: a modelling study. *Lancet Gastroenterol Hepatol*. 2023;8(10):879–907. doi:10.1016/S2468-1253(23)00197-8
29. Therapeutic strategies for hepatitis B virus infection towards a cure.
30. Li Z, Pai R, Gupta S, et al. Presence of onco-fetal neighborhoods in hepatocellular carcinoma is associated with relapse and response to immunotherapy. *Nat Cancer*. 2024;5(1):167–186. doi:10.1038/s43018-023-00672-2
31. Eun JW, Yoon JH, Ahn HR, et al. Cancer-associated fibroblast-derived secreted phosphoprotein 1 contributes to resistance of hepatocellular carcinoma to sorafenib and lenvatinib. *Cancer Commun*. 2023;43(4):455–479. doi:10.1002/cac2.12414
32. Gao J, Li Z, Lu Q, et al. Single-cell RNA sequencing reveals cell subpopulations in the tumor microenvironment contributing to hepatocellular carcinoma. *Front Cell Dev Biol*. 2023;11:1194199. doi:10.3389/fcell.2023.1194199
33. Pitt JM, Marabelle A, Eggermont A, Soria JC, Kroemer G, Zitvogel L. Targeting the tumor microenvironment: removing obstruction to anticancer immune responses and immunotherapy. *Ann Oncol*. 2016;27(8):1482–1492. doi:10.1093/annonc/mdw168
34. Soh BS, Song CM, Vallier L, et al. Pleiotrophin enhances clonal growth and long-term expansion of human embryonic stem cells. *Stem Cells*. 2007;25(12):3029–3037. doi:10.1634/stemcells.2007-0372
35. Sethi G, Kwon Y, Burkhalter RJ, et al. PTN signaling: components and mechanistic insights in human ovarian cancer. *Mol Carcinog*. 2015;54(12):1772–1785. doi:10.1002/mc.22249
36. Shi Y, Ping YF, Zhou W, et al. Tumour-associated macrophages secrete pleiotrophin to promote PTPRZ1 signalling in glioblastoma stem cells for tumour growth. *Nat Commun*. 2017;8:15080. doi:10.1038/ncomms15080
37. Liu S, Shen M, Hsu EC, et al. Discovery of PTN as a serum-based biomarker of pro-metastatic prostate cancer. *Br J Cancer*. 2021;124(5):896–900. doi:10.1038/s41416-020-01200-0
38. Yao J, Zhang C, Chen Y, Gao S. Downregulation of circular RNA circ-LDLRAD3 suppresses pancreatic cancer progression through miR-137-3p/PTN axis. *Life Sci*. 2019;239:116871. doi:10.1016/j.lfs.2019.116871
39. Xu C, Zhu S, Wu M, Han W, Yu Y. Functional receptors and intracellular signal pathways of midkine (MK) and pleiotrophin (PTN). *Biol Pharm Bull*. 2014;37(4):511–520. doi:10.1248/bpb.b13-00845
40. Zhou J, Yang Y, Zhang Y, Liu H, Dou Q. A meta-analysis on the role of pleiotrophin (PTN) as a prognostic factor in cancer. *PLoS One*. 2018;13(11):e0207473. doi:10.1371/journal.pone.0207473
41. Ma J, Kong Y, Nan H, et al. Pleiotrophin as a potential biomarker in breast cancer patients. *Clin Chim Acta*. 2017;466:6–12. doi:10.1016/j.cca.2016.12.030
42. Bai PS, Xia N, Sun H, Kong Y. Pleiotrophin, a target of miR-384, promotes proliferation, metastasis and lipogenesis in HBV-related hepatocellular carcinoma. *J Cell Mol Med*. 2017;21(11):3023–3043. doi:10.1111/jcmm.13213